Draft version June 27, 2024
Typeset using LaTeX twocolumn style in AASTeX631

# Stellar Models are Reliable at Low Metallicity: An Asteroseismic Age for the Ancient Very Metal-Poor Star KIC 8144907

Daniel Huber,[1,2] Ditte Slumstrup,[3,4] Marc Hon,[5,1] Yaguang Li,[1] Victor Aguirre Børsen-Koch,[6] Timothy R. Bedding,[2] Meridith Joyce,[7,8] J. M. Joel Ong,[1] Aldo Serenelli,[9,10] Dennis Stello,[11,2,12] Travis Berger,[13] Samuel K. Grunblatt,[14] Michael Greklek-McKeon,[15] Teruyuki Hirano,[16,17] Evan N. Kirby,[18] Marc H. Pinsonneault,[19] Arthur Alencastro Puls,[20] and Joel Zinn[21]

## ABSTRACT

Very metal-poor stars ([Fe/H] $< -2$) are important laboratories for testing stellar models and reconstructing the formation history of our galaxy. Asteroseismology is a powerful tool to probe stellar interiors and measure ages, but few asteroseismic detections are known in very metal-poor stars and none have allowed detailed modeling of oscillation frequencies. We report the discovery of a low-luminosity *Kepler* red giant (KIC 8144907) with high S/N oscillations, [Fe/H] $= -2.66 \pm 0.08$ and [$\alpha$/Fe] $= 0.38 \pm 0.06$, making it by far the most metal-poor star to date for which detailed asteroseismic modeling is possible. By combining the oscillation spectrum from *Kepler* with high-resolution spectroscopy we measure an asteroseismic mass and age of $0.79 \pm 0.02(\mathrm{ran}) \pm 0.01(\mathrm{sys})\, M_{\odot}$ and $12.0 \pm 0.6(\mathrm{ran}) \pm 0.4(\mathrm{sys})$ Gyr, with remarkable agreement across different codes and input physics, demonstrating that stellar models and asteroseismology are reliable for very metal-poor stars when individual frequencies are used. The results also provide a direct age anchor for the early formation of the Milky Way, implying that substantial star formation did not commence until redshift z$\approx$3 (if the star is part of the ancient galactic disc) or that the Milky Way has undergone merger events for at least $\approx$12 Gyr (if the star was accreted by a dwarf satellite merger such as Gaia Enceladus).

## 1. INTRODUCTION

The study of the chemo-dynamical history of stellar populations in our galaxy is a rapidly evolving field (see e.g. Bland-Hawthorn & Gerhard 2016; Helmi 2020; Bonaca & Price-Whelan 2024, for recent reviews). A particularly important population in our galaxy are metal-poor stars in the Galactic halo, with theories predicting that they formed either through a combination of collapse of gas during the early stages of galaxy formation (Eggen et al. 1962), the accretion of satellite galaxies at later times (Searle & Zinn 1978), a combination of early and late accretion of satellite galaxies (Bullock & Johnston 2005) or ejections of Galactic disc/bulge stars via dynamical interactions (e.g. Purcell et al. 2010).

A key element to advance our understanding of halo stars is stellar ages. The combination of red giant asteroseismology from space-based missions such as *Kepler*, K2 and TESS with spectroscopic surveys such as APOGEE (Holtzman et al. 2015), Gaia-ESO (Gilmore et al. 2012), GALAH (De Silva et al. 2015) and LAMOST (Cui et al. 2012) has provided systematic age constraints for thousands of field red giants (e.g. Miglio et al. 2009; Anders et al. 2017; Stello et al. 2017; Sharma et al. 2019; Montalbán et al. 2021; Borre et al. 2022; Alencastro Puls et al. 2022; Willett et al. 2023; Schonhut-Stasik et al. 2024) and enabled constraints on mass-loss for metal-poor populations in globular clusters (Miglio et al. 2016; Howell et al. 2022; Tailo et al. 2022; Howell et al. 2024). However, all these constraints rely on asteroseismic scaling relations, which are poorly calibrated for metal-poor stars, show systematic offsets compared to expected astrophysical priors for halo stars (Epstein et al. 2014; Matsuno et al. 2021), and yield high random age uncertainties (Moser et al. 2023).

The gold-standard for ages of field stars comes from asteroseismic modeling of individual oscillation frequencies. This "boutique" modeling is often restricted to main-sequence and subgiant stars due to the fast evolution of red giants, which requires more intensive computation. The issue of surface correction also has to be treated carefully (Kjeldsen et al. 2008; Ball et al. 2018; Ong et al. 2021; Li et al. 2023). Because oscillation amplitudes are very small for low-luminosity stars (Bedding 1995; Huber et al. 2011; Mosser et al. 2012; Kallinger

Corresponding author: Daniel Huber
huberd@hawaii.edu

et al. 2014), frequency modeling has been applied only to two stars with [Fe/H] $< -1$: the nearby subgiant $\nu$ Indi ([Fe/H] $= -1.5$ dex), an "in-situ" halo star (Chaplin et al. 2020), and KIC7341231 ([Fe/H] $= -1.6$ dex), which was used to constrain an interior rotation profile (Deheuvels et al. 2012).

Confronting state-of-the-art models with detailed observations at low metallicities has ramifications for a wide range subfields of astrophysics that use stellar models. Asteroseismic frequency modeling of metal-poor stars is important to test these stellar models. For example, prescriptions for convective energy transport in stellar interiors (e.g., Trampedach et al. 2014; Magic et al. 2015; Tayar et al. 2017; Joyce & Chaboyer 2018a; Joyce & Tayar 2023) and the significance of non-local thermodynamic equilibrium (non-LTE) effects in atmospheres (e.g., Bergemann et al. 2012a) depend on metallicity.

Here, we present the results of a survey for metal-poor stars among the *Kepler* oscillating red giant sample. We have found 16 oscillating stars with [Fe/H] $< -1$ and present the first detailed asteroseismic modeling of a very-metal poor star ([Fe/H] $< -2$).

## 2. SPECTROSCOPY

### 2.1. *Survey for Very Metal-Poor Stars*

We performed a spectroscopic survey for very metal-poor stars among known oscillating *Kepler* red giants. Targets were selected from a catalog of oscillating giants with disk height $z > 3$ kpc (Mathur et al. 2016), and by kinematically selecting likely halo stars using Gaia. For the latter, we calculated tangential motions and used a synthetic population from Galaxia (Sharma et al. 2011) to define a fiducial locus of low-luminosity red giants with kinematics that are consistent with halo stars.

Observations were performed between 2017 and 2019 with the Supernova Integrated Field Spectrograph (SNIFS) mounted on UH88 telescope (Lantz et al. 2004), Keck/HIRES (Vogt et al. 1994) and Subaru/HDS (Noguchi et al. 2002). We performed initial low-resolution spectroscopy with SNIFS (R=3000) using template spectra to select candidate very metal-poor stars, which were then followed up with high-resolution spectroscopy. High-resolution spectra were obtained with a typical SNR of 20-40 per pixel, depending on target brightness. An initial abundance analysis was performed using iSpec (Blanco-Cuaresma et al. 2014) with the `spectrum` synthesis code using the wavelength range 600–680 nm. We identified 16 targets as metal-poor ([Fe/H] $< -1$; see Appendix). KIC 8144907 (2MASS J18485977+4401183, $Ks = 11.1$ mag) was identified as a high-priority follow-up target given its rich asteroseismic data from *Kepler* and very low metallicity inferred

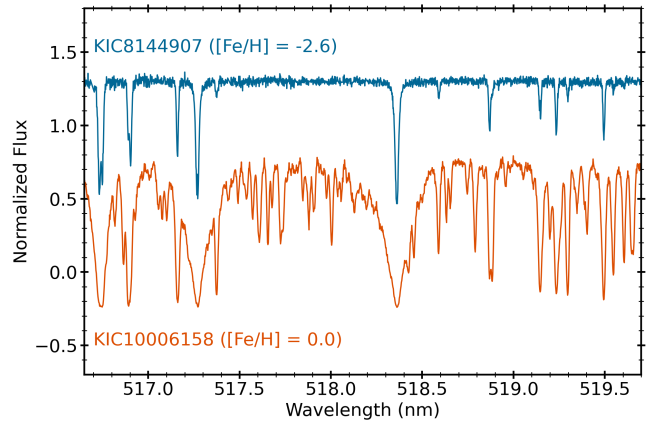


**Figure 1.** Subaru/HDS spectrum of KIC 8144907 near the Mg triplet. The red line shows a Keck/HIRES spectrum of the solar-metallicity star KIC 10006158 for comparison.

from a HIRES spectrum obtained in good conditions on 2019 June 25 with a 300 s exposure and a 1.15" wide slit. We obtained follow-up spectra of KIC 8144907 in 2020 using Subaru/HDS with the I2a setup and the default 0.4" slit, resulting in a spectral resolution of $R \approx 90000$. We co-added spectra with a total integration time of 1.2 hours, resulting in an SNR of 70 between 565–585 nm.

### 2.2. *Atmospheric Parameters and Abundances*

Figure 1 shows a portion of our combined optical spectrum for KIC 8144907 compared to a solar metallicity star. To measure atmospheric parameters and chemical abundances, we used equivalent width measurements while requiring excitation and ionization equilibrium. We varied the temperature until no trend was seen between [Fe/H] and excitation potential while fixing surface gravity to 3.26, as measured from asteroseismic scaling relations (Yu et al. 2018). We ensured agreement between FeI and FeII absorption lines was within one standard deviation. The equivalent widths were measured with DAOSPEC (Stetson & Pancino 2008) and the individual absorption line abundances were calculated with the auxiliary program *Abundance* with SPECTRUM in LTE (Gray & Corbally 1994). The chosen absorption lines and accompanying oscillator strengths are from Slumstrup et al. (2019) for our wavelength range, which is 495–675 nm with a few minor gaps. The solar abundances are those of Grevesse & Sauval (1998) and the stellar atmosphere models are ATLAS9 (Castelli & Kurucz 2004). Due to the very low metallicity we applied non-LTE departure coefficients from the INSPECT database version 1.0[1] (Bergemann et al. 2012b; Lind

[1] available at www.inspect-stars.com

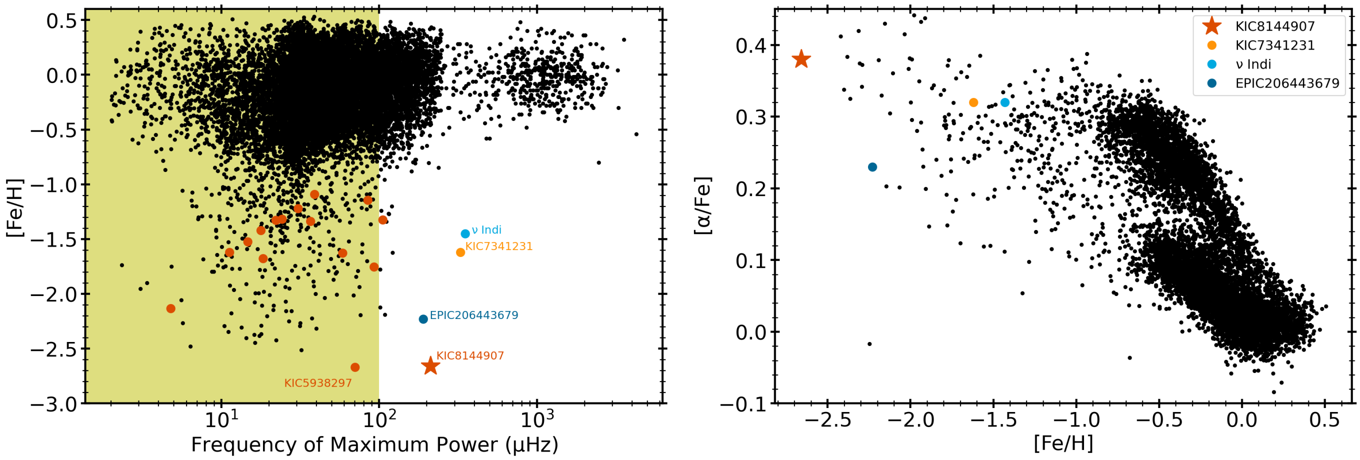


**Figure 2.** Left: Iron abundance versus frequency of maximum power for stars with asteroseismic detections. Literature values (black points) are from Pinsonneault et al. (2014), Serenelli et al. (2017), Matsuno et al. (2021) and Schonhut-Stasik et al. (2024). Individual literature values are from Chaplin et al. (2020) ($\nu$ Indi), Valentini et al. (2019) (EPIC 206443679), and Deheuvels et al. (2014) (KIC7341231). New data from this study are shown as red symbols. The shaded area marks stars generally not amenable to frequency modeling ($\nu_{\rm max} < 100\,\mu$Hz). Right: Same as the left panel but showing $\alpha$ abundance versus metallicity.

et al. 2012) to derive final atmospheric parameters of $T_{\rm eff} = 5400 \pm 200$ K, [Fe/H] $= -2.66 \pm 0.08$ dex and $[\alpha/{\rm Fe}] = 0.38 \pm 0.06$ dex. Uncertainties were calculated by varying each parameter until at least a $3\sigma$ uncertainty is produced on the slope of [Fe/H] vs. excitation potential. We did not detect signs of $r$-process enhancement, such as Eu (which might be expected for Gaia-Enceladus accreted halo stars; Matsuno et al. 2021).

Figure 2 compares KIC 8144907 to known oscillating stars in abundance and frequency space. KIC 8144907 is the most metal-poor oscillating star that is not an evolved red-giant star ($\nu_{\rm max} > 100\,\mu$Hz) and the most metal-poor oscillating star with measured $\alpha$ abundances. EPIC 206443679 (Valentini et al. 2019) is a very metal-poor star with similar $\nu_{\rm max}$, but was only observed for 70 days with K2, limiting the SNR and frequency resolution of the asteroseismic detection. KIC 5938297 is another very metal-poor but more evolved star ($\nu_{\rm max} \approx 80\mu$Hz) identified by our survey.

## 3. ASTEROSEISMOLOGY

### 3.1. *Oscillation Frequencies*

KIC 8144907 was observed by *Kepler* for its entire mission using long-cadence mode. We used the PDC-SAP light curve (Stumpe et al. 2012; Smith et al. 2012) and computed the power spectrum, which shows solar-like oscillations with high SNR (Fig. 3). To extract individual frequencies, we smoothed the spectrum to a resolution of $0.1\,\mu$Hz and measured the positions of the peaks down to a signal-to-noise ratio of 3.5. We identified 49 mode frequencies, which are listed in Table 1.

Figure 3 shows the power spectrum and échelle diagram. Note that the peaks at the top of the échelle diagram are aliases reflected around the Nyquist frequency ($283\,\mu$Hz). The data show clear ridges of radial and quadrupole modes, plus a rich series of mixed dipole modes that are consistent with a star at the base of the RGB. Kuszlewicz et al. (2023) showed that the star has a strongly enhanced mixed-mode coupling strength and rotational splittings that are consistent with the core rotation rates of the general *Kepler* sample.

### 3.2. *Bolometric Flux and Luminosity*

To calculate the bolometric flux ($f_{\rm bol}$) we used 2MASS K-band photometry (Skrutskie et al. 2006) and bolometric corrections from MIST isochrones (Choi et al. 2016), as implemented in `isoclassify` (Huber et al. 2017), interpolated to the spectroscopic $T_{\rm eff}$ , [Fe/H] and asteroseismic $\log g$. Interstellar extinction was calculated using the 3D dustmap from Green et al. (2015), yielding Av=0.15 mag. We assumed uncertainties of 0.03 mag on the bolometric correction and extinction correction (Tayar et al. 2022). We find $f_{\rm bol} = 2.02 \pm 0.06 \times 10^{-10}$ erg s$^{-1}$ cm$^{-2}$, which combined with a distance of $1326 \pm 20$ pc from the *Gaia* DR3 parallax (Gaia Collaboration et al. 2021; Lindegren et al. 2021) yields a luminosity of $11.13 \pm 0.45\,L_{\odot}$.

### 3.3. *Frequency Modeling*

#### 3.3.1. *BeSPP*

A.S. computed models using Garstec (Weiss & Schlattl 2008) with input physics following Serenelli et al. (2017). In summary, nuclear reaction rates are

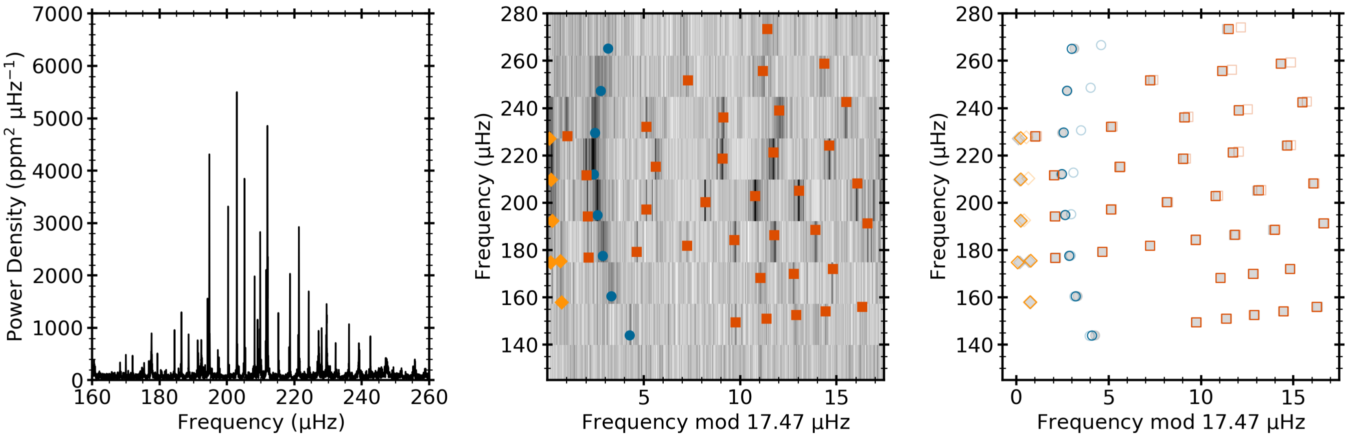


**Figure 3.** *Left:* Power spectrum of the 4-year *Kepler* timeseries of KIC 8144907 centered on the oscillations. *Middle:* Échelle diagram (greyscale) and extracted frequencies for radial (circles), dipole (squares) and quadrupole (diamonds) modes. *Right*: Échelle diagram showing frequencies from the best fitting model before (faint open symbols) and after (open symbols) applying a surface correction. Grey symbols show the observed frequencies.

**Table 1.** Oscillation frequencies and mode identifications for KIC 8144907. We adopt twice the frequency resolution (0.02$\mu$Hz) as a conservative estimate for the uncertainty of each frequency.

| $f(\mu\text{Hz})$ | $l$ | $f(\mu\text{Hz})$ | $l$ | $f(\mu\text{Hz})$ | $l$ |
|---|---|---|---|---|---|
| 144.02 | 0 | 184.40 | 1 | 221.36 | 1 |
| 149.51 | 1 | 186.47 | 1 | 224.25 | 1 |
| 151.11 | 1 | 188.59 | 1 | 227.22 | 2 |
| 152.66 | 1 | 191.30 | 1 | 228.15 | 1 |
| 154.19 | 1 | 192.42 | 2 | 229.59 | 0 |
| 156.07 | 1 | 194.27 | 1 | 232.25 | 1 |
| 157.98 | 2 | 194.78 | 0 | 236.23 | 1 |
| 160.54 | 0 | 197.31 | 1 | 239.13 | 1 |
| 168.27 | 1 | 200.36 | 1 | 242.61 | 1 |
| 170.01 | 1 | 202.94 | 1 | 247.35 | 0 |
| 172.03 | 1 | 205.21 | 1 | 251.87 | 1 |
| 174.88 | 2 | 208.23 | 1 | 255.75 | 1 |
| 175.39 | 2 | 209.83 | 2 | 258.94 | 1 |
| 176.84 | 1 | 211.66 | 1 | 265.19 | 0 |
| 177.57 | 0 | 212.04 | 0 | 273.45 | 1 |
| 179.33 | 1 | 215.25 | 1 | | — |
| 181.94 | 1 | 218.71 | 1 | | — |

from Solar Fusion II (Adelberger et al. 2011), the equation of state is FreeEOS (Irwin 2012), atomic opacities are from OPAL (Iglesias & Rogers 1996), and low-temperature opacities are from the Wichita group (Ferguson et al. 2005). Stellar atmospheres are modeled using a VAL-C T-$\tau$ relation from Vernazza et al. (1981). Mixing length theory is implemented following (Cox & Giuli 1968). The mixing length parameter $\alpha_{\rm MLT} = 1.9980$ is determined consistently by a solar model calibration. Chemical mixing is treated as a diffusive process. Overshooting is modeled following the exponential decay model of Freytag et al. (1996) and a restriction for small convective cores as described by Magic et al. (2010). Gravitational settling is included in the models. In addition, extra-mixing below the convective envelope is included following the parametrization by VandenBerg et al. (2012) with a metallicity dependent calibration of the diffusion coefficient that reproduces the lithium depletion in the Sun and the moderate depletion of metals in old globular clusters.

The model grid covered a mass range between 0.6 and 1.2 $M_\odot$ with a step of 0.01 $M_\odot$, and [Fe/H] between $-1.0$ and $-3.0$. All models have been computed with [$\alpha$/Fe]= 0.4. Evolutionary tracks ran from the Hayashi track to the low-luminosity red giant branch, in practice stopping when the surface gravity reached $\log g = 2.8$. Along each track, about 2000 stellar models were computed. Stellar tracks are pruned to retain only models that are close enough to the surface parameters of the star (within $3\sigma$ for $T_{\rm eff}$ and $6\sigma$ for [Fe/H]) and that have two consecutive radial orders that match (any) two observed radial orders within 4%. The latter implicitly sets an upper limit to the absolute value of the surface corrections for those modes. Then, a fine interpolation is carried out along each pruned track such that the changes in all frequencies within the observed range vary less than the typical observed error.

We assigned a prior probability to each model formed by the product of the timespan each model represents in the track and a weight from assuming a Salpeter initial mass function. We assigned a constant prior to metallicity and star formation rate. Then, to compute the likelihood of each model, we used the reduced $\chi_r^2$, computed as:

$$\chi_r^2 = \frac{1}{N_{\rm obs} - N_{\rm dof}} \sum_{\rm i=1,N_{obs}} \left( \frac{Q_{\rm mod,i} - Q_{\rm obs,i}}{\sigma_{\rm obs,i}} \right)^2, \quad (1)$$

where the first sum extends over $T_{\rm eff}$ , [Fe/H], and $L_\star$, and the oscillation modes (Table 1). Therefore, $N_{\rm obs}$=52. Model frequencies were corrected by surface effects using the two-parameter correction introduced by Ball & Gizon (2014). The number of degrees of freedom in the models is therefore $N_{\rm dof}$=5 (age, mass, [Fe/H] and the two parameters of the surface correction). The likelihood is then proportional to $\exp(-\chi_r^2/2)$. Following these steps, each model was then assigned a probability, which was the product of the prior and likelihood, and probability distribution functions were built for each quantity of interest.

#### 3.3.2. *MESA Model 1*

M.J. used the Modules for Experiments in Stellar Astrophysics (MESA; Paxton et al. 2011, 2013, 2015, 2018, 2019) software suite version 12778 and the GYRE stellar oscillation program (Townsend & Teitler 2013) version 5.2. The physical assumptions adopted in the evolutionary calculations include the Asplund et al. (2009) opacities and solar mixture, the `photosphere_tables` atmospheric boundary conditions, the `'Henyey'` mixing length scheme (Henyey et al. 1965), the `'basic'` nuclear network option, which includes all elements and isotopes necessary for low-mass burning chains up through the helium flash, and the `'exponential'` treatment of convective overshooting, with $f_{\rm ovs} = 0.0014$ times the pressure scale height and primary convective coefficient $f_0 = 0.002$.

Three different fitting schemes for the asteroseismic data were considered: (A) fitting to all modes, including $\ell = 1$; (B) fitting only to $\ell = 0$ and 2 modes; and (C) fitting only to $\ell = 0$ modes. The rank orderings of best-fitting models as determined by methods (B) and (C) were the same. In all cases, the surface corrections of Ball & Gizon (2014) were applied to the frequency fitting, with additional seismic features (e.g. $\nu_{\rm max}, \Delta\nu$ ) calculated according to White et al. (2011).

The fits to individual modes and classical constraints were combined and weighted according to the methods described in Joyce & Chaboyer (2018b) and Murphy et al. (2021).

#### 3.3.3. *MESA Model 2*

D.S. used the astero extension in MESA (v7503) (Paxton et al. 2011, 2013) with the default settings for the model physics, except for the following. We used Asplund et al. (2009) solar abundances, the 'o18_and_ne22' nuclear net, the 'Kunz' C12 rates, and 'jina reaclib' N14 rates. For the outer boundary condition we used the 'photosphere_tables'. For the fitting procedure the non-seismic input observables were effective temperature, luminosity, and metallicity corrected for the star's high alpha element content using the formulation by Salaris et al. (1993). The seismic input was the radial mode frequencies. During model fitting and optimisation, the non-seismic input was weighted 1/3 with 2/3 to the seismic input. We corrected the model frequencies using the 'cubic' formulation by Ball & Gizon (2014), but found no significant difference when using the 'combined' formulation. We set mass, metallicity, and the mixing length parameter as free parameters, while keeping overshoot fixed at 0.015 (exponential prescription). We used an initial helium fraction of 0.248 and an enrichment ratio of 1.4.

#### 3.3.4. *MESA Model 3*

Y.L. used MESA (version r15140) and GYRE (version 5.2), adhering mostly to the default settings, except for specific deviations outlined below. The metal mixture AGSS09 and its corresponding opacities were employed in the models. The Henyey mixing length approach (Henyey et al. 1965) was used for the prescription of convection. Convective overshoot was not incorporated. The atmosphere boundary condition was set to `photosphere tables`, which are pre-calculated model atmosphere tables. A grid of stellar models were calculated with initial helium abundance, stellar mass, metallicity, and the mixing length parameter treated as free parameters. These models were constructed with frequencies and corrected with the surface effect in line with the inverse-cubic method proposed by Ball & Gizon (2014). All models were fitted to the oscillation modes and the classical constraints, including $L$, $T_{\rm eff}$ , and [Fe/H].

#### 3.3.5. *MESA Model 4*

J.M.J.O. constructed MESA models using MESA r12778 and GYRE v6.0. This set of models was constructed with diffusion and settling of helium and metals, an Eddington-gray atmospheric boundary condition, and only a small amount ($f_{\rm ov} = 0.001; f_0 = 0.0005$) of exponential convective overshoot for numerical conditioning. Unlike the other MESA modelling runs, this modelling was also performed with the stellar [Fe/H] computed with respect to the solar chemical abundances of Grevesse & Sauval (1998), with further initial enrichment to match the observational value of [$\alpha$/Fe]. Correspondingly, OPAL opacity tables appropriate to the

GS98 chemical mixture, computed with respect to an alpha-enhancement of $[\alpha/\mathrm{Fe}] = +0.4$, were also adopted. Accordingly, the prescription of Salaris et al. (1993) was *not* used; rather, the actual enriched surface values of [Fe/H] in these models were constrained directly against the observational measurement.

Only modes with confident identifications of $\ell$ were included in the asteroseismic constraint. Radial p-modes were computed using the surface boundary conditions of Christensen-Dalsgaard (2008), and nonradial pure p- and g-mode frequencies, and associated coupling matrices, were computed using the $\pi/\gamma$ isolation scheme of Ong & Basu (2020). The radial and quadrupole p-modes were corrected using the two-term prescription of Ball & Gizon (2014). For the dipole modes, a nonlinear surface term correction was applied (the generalisation to the Ball & Gizon 2014 correction described in Ong et al. 2021), in order to fully account for near-degeneracy avoided crossings between the p- and g-modes, using the same coefficients $a_{-1}$ and $a_3$ as fitted against the even-degree modes. To avoid having to perform the eigendecomposition of a large matrix for every evaluation of the seismic likelihood function, the effective frequency-dependent asymptotic coupling strength $q(\nu)$ was calculated using the expression derived in Ong & Gehan (2023), permitting mixed-mode frequencies to be computed as the roots of the asymptotic eigenvalue equation of e.g. Unno et al. (1979).

The total log-likelihood function we adopted for this exercise was the equally-weighted sum of $\chi^2$ statistics for the observed metallicity, effective temperature, and the luminosity, as well as the reduced $\chi^2$ statistic for the surface-corrected mode frequencies. Maximum-likelihood point estimates were initially derived by minimizing the negative log-likelihood using the differential-evolution algorithm, implemented in Mier (2017), varying the initial mass, helium mass fraction, metal fraction, and mixing length parameter $\alpha_{\mathrm{MLT}}$ as optimisation parameters. Every stellar model constructed along the optimisation trajectory was retained, effectively constituting a nonuniformly sampled grid of stellar models. We then estimate the marginal posterior median and $\pm 1\sigma$ quantiles of the fundamental properties as weighted averages with respect to this grid of models, with the weights being both proportional to the likelihood function, and inversely proportional to the sampling function of the grid (estimated with a kernel density estimator).

#### 3.3.6. *BASTA*

V.A.B.-K. used the BAyesian STellar Algorithm (BASTA) code with a grid of custom models computed using Garstec with input physics as described in Aguirre Børsen-Koch et al. (2022). The grid implements $\alpha$ enhanced and depleted mixtures of the Asplund et al. (2009) solar abundances, ranging from $[\alpha/\mathrm{Fe}] = -0.2$ to 0.6 in steps of 0.1 dex. Oscillation frequencies were calculated using ADIPLS (Christensen-Dalsgaard 2008) with surface corrections following the cubic formulation by Ball & Gizon (2014). Parameter inference follows a Bayesian approach as described by Aguirre Børsen-Koch et al. (2022) and used the spectroscopic constraints ($T_{\mathrm{eff}}$, [Fe/H] and $[\alpha/\mathrm{Fe}]$), Gaia luminosity and observed radial modes.

#### 3.3.7. *Summary*

Table 2 summarizes the properties for KIC 8144907. We observe excellent agreement between modeling methods, with a scatter of ≈2–3% in mass and age. Some methods reported results excluding and including the Gaia luminosity, which were largely consistent, demonstrating that there is no strong disagreement between the luminosities from asteroseismic constraints and Gaia. We adopt self-consistent values from BeSSP, which reported a solution close to the median mass over all methods. For uncertainties, we quote random errors using the mean uncertainty of all methods that fitted non-radial modes and systematic errors as the standard deviation over all methods. Remarkably, the systematic uncertainties for mass and age are a factor of ≈1.5-2 smaller than the random uncertainties. Given the similarity of input physical between methods, the quoted systematic errors only capture part of the uncertainties intrinsic to the models. Possible additional systematic errors may arise from mass loss, but this is expected to be within the uncertainty budget for a star near the base of the RGB. More complete estimates for contributions to the error budget for similar stars have been computed in, e.g., Silva Aguirre et al. (2020); Christensen-Dalsgaard et al. (2020); Tayar et al. (2022); Joyce et al. (2023); Ying et al. (2023).

## 4. IMPLICATIONS FOR MODELS OF VERY METAL-POOR STARS

Metal-poor stars are important testbeds for stellar models. Input physics such as opacities, interior mixing and convective energy transport prescriptions depend on the chemical composition of a star, and become more uncertain for non-solar metallicities (e.g. Joyce & Chaboyer 2018a). The fidelity of such models has a wide impact on astrophysics, including our understanding of galaxies through simple stellar populations models (Conroy et al. 2009).

Our results demonstrate an excellent match between observations and models, including for mixed dipole modes which probe the structure near the core.

**Table 2.** Observed and Derived Properties for KIC 8144907

| | | | | | | | |
|---|---|---|---|---|---|---|---|
| KIC ID & *Kepler* Magnitude | 8144907 | | $Kp = 13.1$ | | | Brown et al. (2011) | |
| Gaia DR3 ID & $G$ Magnitude | 2105367821469848704 | | $G = 12.86$ | | | Lindegren et al. (2021) | |
| 2MASS ID & $K$ magnitude | J18485977+4401183 | | $K = 11.11$ | | | Skrutskie et al. (2006) | |
| Bol. Flux ($10^{-10}\,\mathrm{erg\,s^{-1}\,cm^{-2}}$) | | $2.023 \pm 0.057$ | | | | this work | |
| Luminosity $L$ ($L_\odot$) | | $11.13 \pm 0.45$ | | | | this work | |
| Freq. of max. power $\nu_{\max}$($\mu$Hz) | | $208.2 \pm 1.1$ | | | | Yu et al. (2018) | |
| Large Separation $\Delta\nu$($\mu$Hz) | | $17.47 \pm 0.092$ | | | | Yu et al. (2018) | |
| Period Spacing $\Delta\Pi$ (sec) | | 84.83±0.02 | | | | Kuszlewicz et al. (2023) | |
| Eff. Temperature $T_{\rm eff}$ (K) | | $5400 \pm 200$ | | | | this work | |
| Iron Abundance [Fe/H](dex) | | $-2.66 \pm 0.08$ | | | | this work | |
| Alpha Abundance [$\alpha$/Fe](dex) | | $0.38 \pm 0.06$ | | | | this work | |
| Model | BeSPP | MESA1 | MESA2 | MESA3 | MESA4 | BASTA | Adopted |
| Mass, $M_\star$ ($M_\odot$) | 0.794 | 0.792 | 0.800 | 0.786 | 0.774 | 0.809 | $0.79 \pm 0.02$(ran) $\pm 0.01$(sys) |
| Radius, $R_\star$ ($R_\odot$) | 3.617 | 3.625 | 3.620 | 3.647 | 3.572 | 3.630 | $3.62 \pm 0.04$(ran) $\pm 0.02$(sys) |
| Density, $\rho_\star$ ($10^2\rho_\odot$) | 2.37 | 2.34 | 2.38 | 2.28 | 2.39 | 2.39 | $2.37 \pm 0.02$(ran) $\pm 0.04$(sys) |
| Surface Gravity, $\log g$ (cgs) | 3.221 | 3.218 | 3.223 | 3.210 | 3.221 | 3.226 | $3.221 \pm 0.002$(ran) $\pm 0.006$(sys) |
| Age, t (Gyr) | 11.96 | 12.40 | 12.25 | 12.76 | 12.68 | 11.81 | $12.0 \pm 0.6$(ran) $\pm 0.4$(sys) |

The right panel of Figure 3 compares the best-fitting BeSSP model to the observed oscillating frequencies. The model frequencies agree on average with the observations to within $\approx 0.06\mu$Hz ($\approx 0.03\%$), comparable to modeling results for solar-metallicity stars (e.g. Silva Aguirre et al. 2015). The models also provide a good match to the atmospheric constraints, supporting the fidelity of non-LTE corrections (e.g. Bergemann et al. 2012a), although our $T_{\rm eff}$ uncertainty (200 K) is conservative. Overall, the results imply that state-of-the-art stellar models with standard physical assumptions can reliably reproduce detailed observations of the interior and the atmosphere of a very metal-poor star.

## 5. ASTEROSEISMIC SCALING RELATIONS

Asteroseismic scaling relations use the global oscillation parameters $\nu_{\max}$ and $\Delta\nu$ to calculate fundamental properties by scaling from the Sun. The relations are widely used in the era of ensemble asteroseismology, including to calibrate spectroscopic tracers of stellar mass, which are then used to infer ages with large surveys (Martig et al. 2016; Ho et al. 2017; Ness et al. 2016). Testing scaling relations has become a major subfield of asteroseismology (Huber et al. 2012; Gaulme et al. 2016; Sahlholdt & Silva Aguirre 2018; Themeßl et al. 2018; Zinn 2019; Hekker 2020; Li et al. 2021).

Early results revealed strong inconsistencies between masses from scaling relations and astrophysical expectations for metal-poor stars (Epstein et al. 2014). Several corrections to scaling relations have been proposed (White et al. 2011; Viani et al. 2018). However, all fundamental calibrators to date (such as stars in eclipsing binaries, measured angular diameters, or masses from frequency modeling) have near-solar metallicity. KIC 8144907 provides an opportunity to test scaling relations in the very-metal poor regime.

Using $\nu_{\max}$ and $\Delta\nu$ from Yu et al. (2018), our spectroscopic $T_{\rm eff}$ , and solar reference values from Huber et al. (2011) we calculate a scaling relation mass of $0.98 \pm 0.06 M_\odot$, which is $\approx 24\%$ larger than our adopted mass from individual frequency modeling. Using the corrections of the $\Delta\nu$ scaling relations (Sharma & Stello 2016) calculated by Stello & Sharma (2022) for low-metallicity stars, we obtained $0.99 \pm 0.06 M_\odot$, even higher than the uncorrected values. Recent revisions on the calculated $\Delta\nu$ correction factors due to the surface terms can at most decrease the scaling mass by $\approx$8% (Li et al. 2022; Li et al. 2023), which is still unable to fully explain the difference. This supports a break down of the $\nu_{\max}$ scaling relation in the low-metallicity regime (Belkacem et al. 2011; Zhou et al. 2023) and is in tension with the suggestion that temperature scales are the main cause for overestimated scaling relation masses for metal-poor stars (Schonhut-Stasik et al. 2024).

We also considered the new method of defining and measuring $\nu_{\max}$ introduced by Sreenivas et al. (2024). Using their nuSYD pipeline, they found a value of $\nu_{\max}$ for KIC 8144907 (after correcting for bias) of $209.0 \pm 0.9\,\mu$Hz which, combined with their solar value of $3047\,\mu$Hz, means $\nu_{\max}$ is 0.0686 times solar. This value

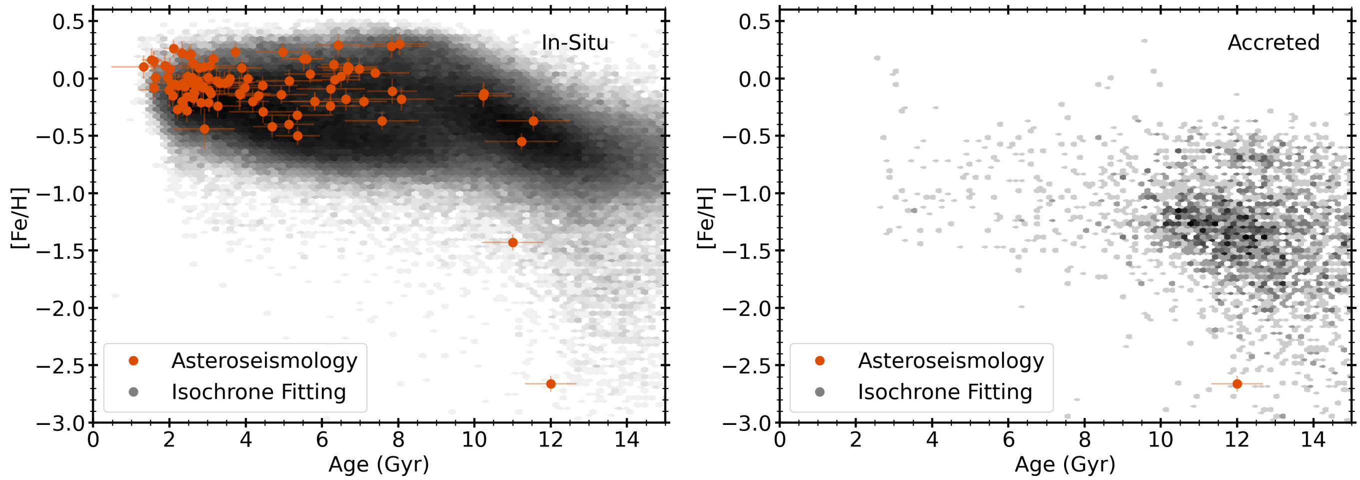


**Figure 4.** Left panel: Iron abundance versus age for stars with ages from detailed asteroseismic modeling (orange circles) and subgiants with ages from isochrone fitting by Xiang & Rix (2022) (grey logarithmic heatmap) with kinematics consistent with an "in-situ" population ($e < 0.8$, $Lz > 0$kpc km s$^{-1}$). Literature asteroseismic ages are taken from Silva Aguirre et al. (2015), Silva Aguirre et al. (2017), Campante et al. (2015), Chaplin et al. (2020) and Li et al. (2020). Right panel: same as left panel but for stars with kinematics consistent with an accreted population ($e > 0.8$, $Lz < -500$kpc km s$^{-1}$). The abundances and kinematics of KIC 8144907 are consistent with either population.

is 2% higher than 0.0674 times solar found by Yu et al. (2018), increasing the mass from the scaling relations by 6% and making the disagreement with the best-fit model even greater.

## 6. AN ASTEROSEISMIC AGE FOR A VERY METAL POOR STAR

KIC 8144907 is consistent with the canonical definition of a local Galactic halo star based on its metallicity ([Fe/H] $< -1$) and kinematics ($|V - V_{\rm LSR}| > 200\,{\rm km\,s^{-1}}$). Gaia led to the discovery that many local stars with halo-like kinematics formed in the Milky Way disc but were later kinematically heated through merger events (Bonaca et al. 2017). At fixed metallicity, such "in-situ" halo stars are generally more enriched in $\alpha$ elements compared to stars that have been accreted from dwarf galaxies that merged with the Milky Way, such as Gaia-Enceladus (Helmi et al. 2018; Belokurov et al. 2018). These low and high $\alpha$ sequences merge for very metal-poor stars, which are rare in Gaia, making the distinction of their origin based on kinematics and chemical abundances more difficult. In general, most stars with [Fe/H] $< -1$ are expected to have been accreted from satellite galaxies (Di Matteo et al. 2019). However, results for high-latitude halo stars have suggested that the oldest Galactic disc stars (the "metal-weak thick disc") can extend to at least [Fe/H] $\approx -2.5$ dex (Carollo et al. 2019; Carter et al. 2021; Conroy et al. 2022), and some very metal-poor stars have also been associated with the oldest stars of the thin disc (Nepal et al. 2024).

To investigate the dynamical origin of KIC 8144907, we compute its orbital kinematics using `galpy` (Bovy 2015) assuming a left-handed Galactocentric coordinate frame with $[V_{R,\odot}, V_{\phi,\odot}, V_{Z,\odot}] = [-12.9, 245.6, 7.78]$ km/s (Drimmel & Poggio 2018), $Z_\odot = 20.8$ pc (Bennett & Bovy 2019), and $R_0 = 8.122$ kpc (GRAVITY Collaboration et al. 2018). The star's orbit is integrated using time-steps of 1 Myr up to a total integration time of 20 Gyr assuming the `McMillan2017` potential (McMillan 2017), which reveals that the star follows an eccentric ($e = 0.75$) orbit with a slight retrograde motion relative to the Milky Way's rotation ($L_z = -0.5 \times 10^3$ kpc km/s). Following Naidu et al. (2020), these chemo-dynamical properties make KIC 8144907 consistent with either the metal-weak thick disc or a Gaia-Enceladus member. Following Feuillet et al. (2020), KIC 8144907 would be classified as a possible Gaia Enceladus member, although its metallicity would be unusually low for that population. The properties of KIC 8144907 also appear consistent with the Atari disk (Mardini et al. 2022), which is suspected to have an accretion origin.

Irrespective of origin, an asteroseismic age for a very metal poor star provides a valuable anchor point for formation events in our galaxy. Figure 4 shows the age-metallicity relation for stars with asteroseismic ages from detailed frequency modeling with uncertainties better than 1 Gyr. We also show a larger sample of subgiant stars with ages determined from isochrone fitting (Xiang & Rix 2022). We divided the sample into likely "in-situ" and "accreted" stars based on eccentricity and angular momentum following Conroy et al. (2022). While this selection is not exact and turn-off ages can be affected by systematic errors due to stellar multiplicity, these cuts give broadly representative distributions. We observe that KIC 8144907 sits at the young edge for both distributions at its metallicity. If KIC 8144907 was formed in-situ and thus belongs the earliest phase of the ancient Galactic disc, its age would imply that substantial star formation in the Milky Way that led to the high-$\alpha$ thick disc did not commence until $\approx$12 Gyr ago (redshift $z \approx 3$). If KIC 8144907 was accreted (e.g., from Gaia Enceladus), it would demonstrate that the Milky Way has undergone merger events for at at least $\approx$12 Gyr. No star with detailed asteroseismic frequency modeling has yet been found to be substantially older than 13 Gyr.

## 7. CONCLUSIONS

We presented the discovery of the most metal-poor star to date for which detailed asteroseismic modeling is possible ([Fe/H] $= -2.66 \pm 0.08$ and [$\alpha$/Fe] $= 0.38 \pm 0.06$). Our main conclusions are as follows:

- We demonstrate that state-of-the-art stellar structure and atmosphere models with non-LTE corrections can successfully reproduce observations of a very metal-poor star, including a large number of oscillation frequencies that probe the stellar core. Masses and ages derived from different methods agree to within $\approx$2-3%, with random errors exceeding systematic errors by a factor of $\approx$1.5-2. This implies that such stellar models make reliable predictions for very metal-poor stellar populations, although we note that not all possible sources of systematic errors were covered in the applied methods.

- We measure a mass of $0.79 \pm 0.02$(ran) $\pm\, 0.01$(sys) $M_{\odot}$, and confirm that asteroseismic scaling relations overestimate stellar masses by $\approx$20% for a very metal-poor star. Corrections to the $\Delta\nu$ relation do not improve the comparison. The results demonstrate that large-scale asteroseismic results based on average seismic parameters (and calibrations that are based on such samples) have to be used with caution for stars with [Fe/H] $< -1$.

- We measure an age of $12.0 \pm 0.6$(ran) $\pm\, 0.4$(sys) Gyr, the first such estimate from detailed asteroseismic modeling for a very metal-poor star. The chemical abundances and kinematics of the star are consistent with either an ancient Galactic disc star (implying that substantial star formation in the Galaxy did not commence until $z \approx 3$) or with being accreted from a dwarf satellite such as Gaia Enceladus (implying that Milky Way has undergone merger events for at least 12 Gyr).

KIC 8144907 demonstrates the value of systematic spectroscopic follow-up for stars with asteroseismic detections from space-based telescopes, in particular those with high S/N detections from *Kepler* and in the TESS continuous viewing zones. Accumulating more examples will be critical for the success of Galactic archeology, in particular for improving the reliability spectroscopic age scales that are calibrated on asteroseismology (e.g. Martig et al. 2016). Given the large number of projected asteroseismic detections from TESS (Hon et al. 2021, e.g.), this will require large-scale spectroscopic surveys such as SDSS-V (Kollmeier et al. 2017), 4MOST (de Jong et al. 2012), WEAVE (Dalton et al. 2012) MSE (The MSE Science Team et al. 2019; Bergemann et al. 2019) and WST (Bacon et al. 2024).

Data and code to reproduce all figures in this paper can be found at https://github.com/danxhuber/very-metal-poor-seismology. The *Kepler* data used in this paper can be found in MAST: 10.17909/xsvn-fe82.

The authors wish to recognize and acknowledge the very significant cultural role and reverence that the summit of Maunakea has always had within the Native Hawaiian community. We are most fortunate to have the opportunity to conduct observations from this mountain.

Some of the data presented herein were obtained at Keck Observatory, which is a private 501(c)3 non-profit organization operated as a scientific partnership among the California Institute of Technology, the University of California, and the National Aeronautics and Space Administration. The Observatory was made possible by the generous financial support of the W. M. Keck Foundation. This research is based in part on data collected at the Subaru Telescope, which is operated by the National Astronomical Observatory of Japan.

D.H. acknowledges support from the Alfred P. Sloan Foundation, the National Aeronautics and Space Administration (80NSSC19K0597), and the Australian Research Council (FT200100871). A.S. acknowledges grants Spanish program Unidad de Excelencia María de Maeztu CEX2020-001058-M, 2021-SGR-1526 (Generalitat de Catalunya), and support from ChETEC-INFRA (EU project no. 101008324). D.S. is supported by the Australian Research Council (DP190100666). E.N.K. acknowledges support from NSF CAREER grant AST-2233781. T.R.B. acknowledges support from the Australian Research Council through Laureate Fellowship FL220100117. M.J. gratefully acknowledges funding of MATISSE: *Measuring Ages Through Isochrones, Seismology, and Stellar Evolution*, awarded through the European Commission's Widening Fellowship. This project has received funding from the European Union's Horizon 2020 research and innovation programme. A.A.P. acknowledges the support by the State of Hesse within the Research Cluster ELEMENTS (Project ID 500/10.006). This research was supported by the Munich Institute for Astro-, Particle and BioPhysics (MIAPbP) which is funded by the Deutsche Forschungsgemeinschaft (DFG, German Research Foundation) under Germany´s Excellence Strategy – EXC-2094 – 390783311.

*Software:* This research made use of echelle (Hey & Ball 2020), isoclassify (Huber et al. 2017; Berger et al. 2020), Lightkurve (Lightkurve Collaboration et al. 2018), Matplotlib (Hunter 2007), numpy (Harris et al. 2020) and scipy (Virtanen et al. 2020).

*Facilities:* UH:2.2m, Keck, Subaru, Kepler

# APPENDIX

## A. METAL POOR STAR CATALOG

**Table 3.** Metal poor oscillating Kepler red giants

| KIC | $\nu_{\rm max}$ | [Fe/H] |
|---|---|---|
| 5522939 | 22.1 | -1.3 |
| 5938297 | 70.5 | -2.7 |
| 6278241 | 14.7 | -1.5 |
| 7259558 | 24.2 | -1.3 |
| 7635173 | 30.7 | -1.2 |
| 7660280 | 36.7 | -1.3 |
| 7879709 | 18.4 | -1.7 |
| 8411296 | 11.3 | -1.6 |
| 8611078 | 58.7 | -1.6 |
| 9508233 | 39.0 | -1.1 |
| 10728519 | 84.9 | -1.1 |
| 11445766 | 17.8 | -1.4 |
| 11460115 | 105.5 | -1.3 |
| 11700922 | 4.8 | -2.1 |
| 11704816 | 92.9 | -1.8 |

Notes: Other stars found to be metal-poor ([Fe/H] $< -1$) by our spectroscopic survey. $\nu_{\rm max}$ values are taken from Yu et al. (2018), [Fe/H] values were derived using iSpec. Uncertainties on [Fe/H] are $\approx 0.1$ dex based on a comparison to metallicities derived from APOGEE for a subset of stars.

# REFERENCES

Adelberger, E. G., García, A., Robertson, R. G. H., et al. 2011, Reviews of Modern Physics, 83, 195, doi: 10.1103/RevModPhys.83.195

Aguirre Børsen-Koch, V., Rørsted, J. L., Justesen, A. B., et al. 2022, Monthly Notices of the Royal Astronomical Society, 509, 4344, doi: 10.1093/mnras/stab2911

Alencastro Puls, A., Casagrande, L., Monty, S., et al. 2022, Monthly Notices of the Royal Astronomical Society, 510, 1733, doi: 10.1093/mnras/stab3545

Anders, F., Chiappini, C., Rodrigues, T. S., et al. 2017, Astronomy and Astrophysics, 597, A30, doi: 10.1051/0004-6361/201527204

Asplund, M., Grevesse, N., Sauval, A. J., & Scott, P. 2009, Annual Review of Astronomy and Astrophysics, 47, 481, doi: 10.1146/annurev.astro.46.060407.145222

Bacon, R., Maineiri, V., Randich, S., et al. 2024, WST – Widefield Spectroscopic Telescope: Motivation, science drivers and top-level requirements for a new dedicated facility, doi: 10.48550/arXiv.2405.12518

Ball, W. H., & Gizon, L. 2014, Astronomy and Astrophysics, 568, A123, doi: 10.1051/0004-6361/201424325

Ball, W. H., & Gizon, L. 2014, A&A, 568, A123, doi: 10.1051/0004-6361/201424325

Ball, W. H., Themeßl, N., & Hekker, S. 2018, Monthly Notices of the Royal Astronomical Society, 478, 4697, doi: 10.1093/mnras/sty1141

Bedding, K. . 1995, Amplitude of stellar oscillations: the implications for Asteroseismology

Belkacem, K., Goupil, M. J., Dupret, M. A., et al. 2011, Astronomy & Astrophysics, 530, A142, doi: 10.1051/0004-6361/201116490

Belokurov, V., Erkal, D., Evans, N. W., Koposov, S. E., & Deason, A. J. 2018, MNRAS, 478, 611, doi: 10.1093/mnras/sty982

Bennett, M., & Bovy, J. 2019, MNRAS, 482, 1417, doi: 10.1093/mnras/sty2813

Bergemann, M., Lind, K., Collet, R., Magic, Z., & Asplund, M. 2012a, Monthly Notices of the Royal Astronomical Society, 427, 27, doi: 10.1111/j.1365-2966.2012.21687.x

—. 2012b, MNRAS, 427, 27, doi: 10.1111/j.1365-2966.2012.21687.x

Bergemann, M., Huber, D., Adibekyan, V., et al. 2019, arXiv:1903.03157 [astro-ph]. http://arxiv.org/abs/1903.03157

Berger, T. A., Huber, D., van Saders, J. L., et al. 2020, The Astronomical Journal, 159, 280, doi: 10.3847/1538-3881/159/6/280

Blanco-Cuaresma, S., Soubiran, C., Heiter, U., & Jofré, P. 2014, Astronomy and Astrophysics, 569, A111, doi: 10.1051/0004-6361/201423945

Bland-Hawthorn, J., & Gerhard, O. 2016, Annual Review of Astronomy and Astrophysics, 54, 529, doi: 10.1146/annurev-astro-081915-023441

Bonaca, A., Conroy, C., Wetzel, A., Hopkins, P. F., & Kereš, D. 2017, The Astrophysical Journal, 845, 101, doi: 10.3847/1538-4357/aa7d0c

Bonaca, A., & Price-Whelan, A. M. 2024, Stellar Streams in the Gaia Era, doi: 10.48550/arXiv.2405.19410

Borre, C. C., Aguirre Børsen-Koch, V., Helmi, A., et al. 2022, Monthly Notices of the Royal Astronomical Society, 514, 2527, doi: 10.1093/mnras/stac1498

Bovy, J. 2015, ApJS, 216, 29, doi: 10.1088/0067-0049/216/2/29

Brown, T. M., Latham, D. W., Everett, M. E., & Esquerdo, G. A. 2011, The Astronomical Journal, 142, 112, doi: 10.1088/0004-6256/142/4/112

Bullock, J. S., & Johnston, K. V. 2005, The Astrophysical Journal, 635, 931, doi: 10.1086/497422

Campante, T. L., Barclay, T., Swift, J. J., et al. 2015, The Astrophysical Journal, 799, 170, doi: 10.1088/0004-637X/799/2/170

Carollo, D., Chiba, M., Ishigaki, M., et al. 2019, The Astrophysical Journal, 887, 22, doi: 10.3847/1538-4357/ab517c

Carter, C., Conroy, C., Zaritsky, D., et al. 2021, The Astrophysical Journal, 908, 208, doi: 10.3847/1538-4357/abcda4

Castelli, F., & Kurucz, R. L. 2004, ArXiv e-prints \rm (arXiv:0405087)

Chaplin, W. J., Serenelli, A. M., Miglio, A., et al. 2020, Nature Astronomy, 4, 382, doi: 10.1038/s41550-019-0975-9

Choi, J., Dotter, A., Conroy, C., et al. 2016, The Astrophysical Journal, 823, 102, doi: 10.3847/0004-637X/823/2/102

Christensen-Dalsgaard, J. 2008, Astrophysics and Space Science, 316, 113, doi: 10.1007/s10509-007-9689-z

Christensen-Dalsgaard, J., Silva Aguirre, V., Cassisi, S., et al. 2020, Astronomy and Astrophysics, 635, A165, doi: 10.1051/0004-6361/201936766

Conroy, C., Gunn, J. E., & White, M. 2009, The Astrophysical Journal, 699, 486, doi: 10.1088/0004-637X/699/1/486

Conroy, C., Weinberg, D. H., Naidu, R. P., et al. 2022, Birth of the Galactic Disk Revealed by the H3 Survey, arXiv. http://arxiv.org/abs/2204.02989

Cox, J. P., & Giuli, R. T. 1968, Principles of stellar structure (Gordon and Breach: New York)

Cui, X.-Q., Zhao, Y.-H., Chu, Y.-Q., et al. 2012, Research in Astronomy and Astrophysics, 12, 1197, doi: 10.1088/1674-4527/12/9/003

Dalton, G., Trager, S. C., Abrams, D. C., et al. 2012, 8446, 84460P, doi: 10.1117/12.925950

de Jong, R. S., Bellido-Tirado, O., Chiappini, C., et al. 2012, 8446, 84460T, doi: 10.1117/12.926239

De Silva, G. M., Freeman, K. C., Bland-Hawthorn, J., et al. 2015, Monthly Notices of the Royal Astronomical Society, 449, 2604, doi: 10.1093/mnras/stv327

Deheuvels, S., García, R. A., Chaplin, W. J., et al. 2012, The Astrophysical Journal, 756, 19, doi: 10.1088/0004-637X/756/1/19

Deheuvels, S., Doğan, G., Goupil, M. J., et al. 2014, Astronomy and Astrophysics, 564, A27, doi: 10.1051/0004-6361/201322779
Di Matteo, P., Haywood, M., Lehnert, M. D., et al. 2019, Astronomy & Astrophysics, 632, A4, doi: 10.1051/0004-6361/201834929
Drimmel, R., & Poggio, E. 2018, Research Notes of the American Astronomical Society, 2, 210, doi: 10.3847/2515-5172/aaef8b
Eggen, O. J., Lynden-Bell, D., & Sandage, A. R. 1962, The Astrophysical Journal, 136, 748, doi: 10.1086/147433
Epstein, C. R., Elsworth, Y. P., Johnson, J. A., et al. 2014, The Astrophysical Journal, 785, L28, doi: 10.1088/2041-8205/785/2/L28
Ferguson, J. W., Alexander, D. R., Allard, F., et al. 2005, The Astrophysical Journal, 623, 585, doi: 10.1086/428642
Feuillet, D. K., Feltzing, S., Sahlholdt, C. L., & Casagrande, L. 2020, MNRAS, 497, 109, doi: 10.1093/mnras/staa1888
Freytag, B., Ludwig, H. G., & Steffen, M. 1996, Astronomy and Astrophysics, 313, 497. https://ui.adsabs.harvard.edu/abs/1996A&A...313..497F
Gaia Collaboration, Brown, A. G. A., Vallenari, A., et al. 2021, Astronomy and Astrophysics, 649, A1, doi: 10.1051/0004-6361/202039657
Gaulme, P., McKeever, J., Jackiewicz, J., et al. 2016, The Astrophysical Journal, 832, 121, doi: 10.3847/0004-637X/832/2/121
Gilmore, G., Randich, S., Asplund, M., et al. 2012, The Messenger, 147, 25. http://adsabs.harvard.edu/abs/2012Msngr.147...25G
GRAVITY Collaboration, Abuter, R., Amorim, A., et al. 2018, A&A, 615, L15, doi: 10.1051/0004-6361/201833718
Gray, R. O., & Corbally, C. J. 1994, AJ, 107, 742, doi: 10.1086/116893
Green, G. M., Schlafly, E. F., Finkbeiner, D. P., et al. 2015, The Astrophysical Journal, 810, 25, doi: 10.1088/0004-637X/810/1/25
Grevesse, N., & Sauval, A. J. 1998, Standard solar composition, doi: 10.1023/A:1005161325181
Grevesse, N., & Sauval, A. J. 1998, SSRv, 85, 161, doi: 10.1023/A:1005161325181
Harris, C. R., Millman, K. J., Walt, S. J. v. d., et al. 2020, Nature, 585, 357, doi: 10.1038/s41586-020-2649-2
Hekker, S. 2020, Frontiers in Astronomy and Space Sciences, 7, 3, doi: 10.3389/fspas.2020.00003
Helmi, A. 2020, Annual Review of Astronomy and Astrophysics, 58, 205, doi: 10.1146/annurev-astro-032620-021917
Helmi, A., Babusiaux, C., Koppelman, H. H., et al. 2018, Nature, 563, 85, doi: 10.1038/s41586-018-0625-x
Henyey, L., Vardya, M. S., & Bodenheimer, P. 1965, ApJ, 142, 841, doi: 10.1086/148357
Hey, D., & Ball, W. 2020, Echelle: Dynamic echelle diagrams for asteroseismology, Zenodo, doi: 10.5281/zenodo.3629933
Ho, A. Y. Q., Rix, H.-W., Ness, M. K., et al. 2017, The Astrophysical Journal, 841, 40, doi: 10.3847/1538-4357/aa6db3
Holtzman, J. A., Shetrone, M., Johnson, J. A., et al. 2015, The Astronomical Journal, 150, 148, doi: 10.1088/0004-6256/150/5/148
Hon, M., Huber, D., Kuszlewicz, J. S., et al. 2021, The Astrophysical Journal, 919, 131, doi: 10.3847/1538-4357/ac14b1
Howell, M., Campbell, S. W., Stello, D., & De Silva, G. M. 2022, Monthly Notices of the Royal Astronomical Society, 515, 3184, doi: 10.1093/mnras/stac1918
—. 2024, Monthly Notices of the Royal Astronomical Society, 527, 7974, doi: 10.1093/mnras/stad3565
Huber, D., Bedding, T. R., Arentoft, T., et al. 2011, The Astrophysical Journal, 731, 94, doi: 10.1088/0004-637X/731/2/94
Huber, D., Ireland, M. J., Bedding, T. R., et al. 2012, The Astrophysical Journal, 760, 32, doi: 10.1088/0004-637X/760/1/32
Huber, D., Zinn, J., Bojsen-Hansen, M., et al. 2017, The Astrophysical Journal, 844, 102, doi: 10.3847/1538-4357/aa75ca
Hunter, J. D. 2007, Computing in Science & Engineering, 9, 90, doi: 10.1109/MCSE.2007.55
Iglesias, C. A., & Rogers, F. J. 1996, ApJ, 464, 943, doi: 10.1086/177381
Irwin, A. W. 2012, FreeEOS: Equation of State for stellar interiors calculations, Astrophysics Source Code Library, record ascl:1211.002
Joyce, M., & Chaboyer, B. 2018a, ApJ, 856, 10, doi: 10.3847/1538-4357/aab200
—. 2018b, ApJ, 864, 99, doi: 10.3847/1538-4357/aad464
Joyce, M., Johnson, C. I., Marchetti, T., et al. 2023, ApJ, 946, 28, doi: 10.3847/1538-4357/acb692
Joyce, M., & Tayar, J. 2023, Galaxies, 11, 75, doi: 10.3390/galaxies11030075
Kallinger, T., De Ridder, J., Hekker, S., et al. 2014, Astronomy & Astrophysics, 570, A41, doi: 10.1051/0004-6361/201424313
Kjeldsen, H., Bedding, T. R., & Christensen-Dalsgaard, J. 2008, \apjl, 683, L175, doi: 10.1086/591667
Kollmeier, J. A., Zasowski, G., Rix, H.-W., et al. 2017, SDSS-V: Pioneering Panoptic Spectroscopy, doi: 10.48550/arXiv.1711.03234

Kuszlewicz, J. S., Hon, M., & Huber, D. 2023, The Astrophysical Journal, 954, 152, doi: 10.3847/1538-4357/ace598

Lantz, B., Aldering, G., Antilogus, P., et al. 2004, 5249, 146, doi: 10.1117/12.512493

Li, T., Bedding, T. R., Christensen-Dalsgaard, J., et al. 2020, Monthly Notices of the Royal Astronomical Society, 495, 3431, doi: 10.1093/mnras/staa1350

Li, T., Li, Y., Bi, S., et al. 2022, ApJ, 927, 167, doi: 10.3847/1538-4357/ac4fbf

Li, Y., Bedding, T. R., Stello, D., et al. 2021, MNRAS, 501, 3162, doi: 10.1093/mnras/staa3932

Li, Y., Bedding, T. R., Stello, D., et al. 2023, Monthly Notices of the Royal Astronomical Society, 523, 916, doi: 10.1093/mnras/stad1445

Lightkurve Collaboration, Cardoso, J. V. d. M., Hedges, C., et al. 2018, Lightkurve: Kepler and TESS time series analysis in Python

Lind, K., Bergemann, M., & Asplund, M. 2012, MNRAS, 427, 50, doi: 10.1111/j.1365-2966.2012.21686.x

Lindegren, L., Klioner, S. A., Hernández, J., et al. 2021, Astronomy and Astrophysics, 649, A2, doi: 10.1051/0004-6361/202039709

Magic, Z., Chiavassa, A., Collet, R., & Asplund, M. 2015, Astronomy and Astrophysics, 573, A90, doi: 10.1051/0004-6361/201423804

Magic, Z., Serenelli, A., Weiss, A., & Chaboyer, B. 2010, ApJ, 718, 1378, doi: 10.1088/0004-637X/718/2/1378

Mardini, M. K., Frebel, A., Chiti, A., et al. 2022, The Astrophysical Journal, 936, 78, doi: 10.3847/1538-4357/ac8102

Martig, M., Fouesneau, M., Rix, H.-W., et al. 2016, MNRAS, 456, 3655, doi: 10.1093/mnras/stv2830

Mathur, S., García, R. A., Huber, D., et al. 2016, The Astrophysical Journal, 827, 50, doi: 10.3847/0004-637X/827/1/50

Matsuno, T., Hirai, Y., Tarumi, Y., et al. 2021, A&A, 650, A110, doi: 10.1051/0004-6361/202040227

Matsuno, T., Aoki, W., Casagrande, L., et al. 2021, The Astrophysical Journal, 912, 72, doi: 10.3847/1538-4357/abeab2

McMillan, P. J. 2017, MNRAS, 465, 76, doi: 10.1093/mnras/stw2759

Mier, P. R. 2017, pablormier/yabox: v1.0.3, v1.0.3, Zenodo, doi: 10.5281/zenodo.848679

Miglio, A., Montalbán, J., Baudin, F., et al. 2009, Astronomy & Astrophysics, 503, L21, doi: 10.1051/0004-6361/200912822

Miglio, A., Chaplin, W. J., Brogaard, K., et al. 2016, Monthly Notices of the Royal Astronomical Society, 461, 760, doi: 10.1093/mnras/stw1555

Montalbán, J., Mackereth, J. T., Miglio, A., et al. 2021, Nature Astronomy, 5, 640, doi: 10.1038/s41550-021-01347-7

Moser, S., Valle, G., Dell'Omodarme, M., Degl'Innocenti, S., & Prada Moroni, P. G. 2023, Astronomy and Astrophysics, 671, A78, doi: 10.1051/0004-6361/202243897

Mosser, B., Elsworth, Y., Hekker, S., et al. 2012, Astronomy & Astrophysics, 537, A30, doi: 10.1051/0004-6361/201117352

Murphy, S. J., Joyce, M., Bedding, T. R., White, T. R., & Kama, M. 2021, MNRAS, 502, 1633, doi: 10.1093/mnras/stab144

Naidu, R. P., Conroy, C., Bonaca, A., et al. 2020, The Astrophysical Journal, 901, 48, doi: 10.3847/1538-4357/abaef4

Nepal, S., Chiappini, C., Queiroz, A. B. A., et al. 2024, Discovery of the local counterpart of disc galaxies at z > 4: The oldest thin disc of the Milky Way using Gaia-RVS, doi: 10.48550/arXiv.2402.00561

Ness, M., Hogg, D. W., Rix, H. W., et al. 2016, The Astrophysical Journal, 823, 114, doi: 10.3847/0004-637X/823/2/114

Noguchi, K., Aoki, W., Kawanomoto, S., et al. 2002, Publications of the Astronomical Society of Japan, 54, 855, doi: 10.1093/pasj/54.6.855

Ong, J. M. J., & Basu, S. 2020, ApJ, 898, 127, doi: 10.3847/1538-4357/ab9ffb

Ong, J. M. J., Basu, S., & Roxburgh, I. W. 2021, The Astrophysical Journal, 920, 8, doi: 10.3847/1538-4357/ac12ca

Ong, J. M. J., & Gehan, C. 2023, ApJ, 946, 92, doi: 10.3847/1538-4357/acbf2f

Paxton, B., Bildsten, L., Dotter, A., et al. 2011, The Astrophysical Journal Supplement Series, 192, 3, doi: 10.1088/0067-0049/192/1/3

Paxton, B., Cantiello, M., Arras, P., et al. 2013, The Astrophysical Journal Supplement Series, 208, 4, doi: 10.1088/0067-0049/208/1/4

Paxton, B., Marchant, P., Schwab, J., et al. 2015, The Astrophysical Journal Supplement Series, 220, 15, doi: 10.1088/0067-0049/220/1/15

Paxton, B., Schwab, J., Bauer, E. B., et al. 2018, The Astrophysical Journal Supplement Series, 234, 34, doi: 10.3847/1538-4365/aaa5a8

Paxton, B., Smolec, R., Schwab, J., et al. 2019, The Astrophysical Journal Supplement Series, 243, 10, doi: 10.3847/1538-4365/ab2241

Pinsonneault, M. H., Elsworth, Y., Epstein, C., et al. 2014, The Astrophysical Journal Supplement Series, 215, 19, doi: 10.1088/0067-0049/215/2/19

Purcell, C. W., Bullock, J. S., & Kazantzidis, S. 2010, Monthly Notices of the Royal Astronomical Society, 404, 1711, doi: 10.1111/j.1365-2966.2010.16429.x

Sahlholdt, C. L., & Silva Aguirre, V. 2018, Monthly Notices of the Royal Astronomical Society, 481, L125, doi: 10.1093/mnrasl/sly173

Salaris, M., Chieffi, A., & Straniero, O. 1993, The Astrophysical Journal, 414, 580, doi: 10.1086/173105

Schonhut-Stasik, J., Zinn, J. C., Stassun, K. G., et al. 2024, AJ, 167, 50, doi: 10.3847/1538-3881/ad0b13

Searle, L., & Zinn, R. 1978, The Astrophysical Journal, 225, 357, doi: 10.1086/156499

Serenelli, A., Johnson, J., Huber, D., et al. 2017, The Astrophysical Journal Supplement Series, 233, 23, doi: 10.3847/1538-4365/aa97df

Sharma, S., Bland-Hawthorn, J., Johnston, K. V., & Binney, J. 2011, The Astrophysical Journal, 730, 3, doi: 10.1088/0004-637X/730/1/3

Sharma, S., & Stello, D. 2016, Astrophysics Source Code Library, ascl:1603.009. https://ui.adsabs.harvard.edu/abs/2016ascl.soft03009S

Sharma, S., Stello, D., Bland-Hawthorn, J., et al. 2019, Monthly Notices of the Royal Astronomical Society, 490, 5335, doi: 10.1093/mnras/stz2861

Silva Aguirre, V., Davies, G. R., Basu, S., et al. 2015, Monthly Notices of the Royal Astronomical Society, 452, 2127, doi: 10.1093/mnras/stv1388

Silva Aguirre, V., Lund, M. N., Antia, H. M., et al. 2017, The Astrophysical Journal, 835, 173, doi: 10.3847/1538-4357/835/2/173

Silva Aguirre, V., Christensen-Dalsgaard, J., Cassisi, S., et al. 2020, Astronomy and Astrophysics, 635, A164, doi: 10.1051/0004-6361/201935843

Skrutskie, M. F., Cutri, R. M., Stiening, R., et al. 2006, The Astronomical Journal, 131, 1163, doi: 10.1086/498708

Slumstrup, D., Grundahl, F., Silva Aguirre, V., & Brogaard, K. 2019, A&A, 622, A111, doi: 10.1051/0004-6361/201833739

Smith, J. C., Stumpe, M. C., Van Cleve, J. E., et al. 2012, Publications of the Astronomical Society of the Pacific, 124, 1000, doi: 10.1086/667697

Sreenivas, K. R., Bedding, T. R., Li, Y., et al. 2024, MNRAS, doi: 10.1093/mnras/stae991

Stello, D., & Sharma, S. 2022, Research Notes of the American Astronomical Society, 6, 168, doi: 10.3847/2515-5172/ac8b12

Stello, D., Zinn, J., Elsworth, Y., et al. 2017, \apj, 835, 83, doi: 10.3847/1538-4357/835/1/83

Stetson, P. B., & Pancino, E. 2008, PASP, 120, 1332, doi: 10.1086/596126

Stumpe, M. C., Smith, J. C., Van Cleve, J. E., et al. 2012, Publications of the Astronomical Society of the Pacific, 124, 985, doi: 10.1086/667698

Tailo, M., Corsaro, E., Miglio, A., et al. 2022, Astronomy and Astrophysics, 662, L7, doi: 10.1051/0004-6361/202243721

Tayar, J., Claytor, Z. R., Huber, D., & van Saders, J. 2022, The Astrophysical Journal, 927, 31, doi: 10.3847/1538-4357/ac4bbc

Tayar, J., Somers, G., Pinsonneault, M. H., et al. 2017, ApJ, 840, 17, doi: 10.3847/1538-4357/aa6a1e

The MSE Science Team, Babusiaux, C., Bergemann, M., et al. 2019, The Detailed Science Case for the Maunakea Spectroscopic Explorer, 2019 edition, doi: 10.48550/arXiv.1904.04907

Themeßl, N., Hekker, S., Southworth, J., et al. 2018, Monthly Notices of the Royal Astronomical Society, 478, 4669, doi: 10.1093/mnras/sty1113

Townsend, R. H. D., & Teitler, S. A. 2013, Monthly Notices of the Royal Astronomical Society, 435, 3406, doi: 10.1093/mnras/stt1533

Trampedach, R., Stein, R. F., Christensen-Dalsgaard, J., Nordlund, , & Asplund, M. 2014, Monthly Notices of the Royal Astronomical Society, 445, 4366, doi: 10.1093/mnras/stu2084

Unno, W., Osaki, Y., Ando, H., & Shibahashi, H. 1979, Nonradial oscillations of stars

Valentini, M., Chiappini, C., Bossini, D., et al. 2019, Astronomy & Astrophysics, 627, A173, doi: 10.1051/0004-6361/201834081

VandenBerg, D. A., Bergbusch, P. A., Dotter, A., et al. 2012, ApJ, 755, 15, doi: 10.1088/0004-637X/755/1/15

Vernazza, J. E., Avrett, E. H., & Loeser, R. 1981, ApJS, 45, 635, doi: 10.1086/190731

Viani, L. S., Basu, S., Ong J., M. J., Bonaca, A., & Chaplin, W. J. 2018, The Astrophysical Journal, 858, 28, doi: 10.3847/1538-4357/aab7eb

Virtanen, P., Gommers, R., Oliphant, T. E., et al. 2020, Nature Methods, 17, 261, doi: 10.1038/s41592-019-0686-2

Vogt, S. S., Allen, S. L., Bigelow, B. C., et al. 1994, in Society of Photo-Optical Instrumentation Engineers (SPIE) Conference Series, Vol. 2198, Society of Photo-Optical Instrumentation Engineers (SPIE) Conference Series, ed. D. L. Crawford & E. R. Craine, 362

Weiss, A., & Schlattl, H. 2008, Ap&SS, 316, 99, doi: 10.1007/s10509-007-9606-5

White, T. R., Bedding, T. R., Stello, D., et al. 2011, ApJ, 743, 161, doi: 10.1088/0004-637X/743/2/161

White, T. R., Bedding, T. R., Stello, D., et al. 2011, The Astrophysical Journal, 742, L3, doi: 10.1088/2041-8205/742/1/L3

Willett, E., Miglio, A., Mackereth, J. T., et al. 2023, Monthly Notices of the Royal Astronomical Society, 526, 2141, doi: 10.1093/mnras/stad2374

Xiang, M., & Rix, H.-W. 2022, Nature, 603, 599, doi: 10.1038/s41586-022-04496-5

Ying, J. M., Chaboyer, B., Boudreaux, E. M., et al. 2023, AJ, 166, 18, doi: 10.3847/1538-3881/acd9b1

Yu, J., Huber, D., Bedding, T. R., et al. 2018, The Astrophysical Journal Supplement Series, 236, 42, doi: 10.3847/1538-4365/aaaf74

Zhou, Y., Christensen-Dalsgaard, J., Asplund, M., et al. 2023, arXiv e-prints, arXiv:2310.20050, doi: 10.48550/arXiv.2310.20050

Zinn, J. C. 2019, The Astrophysical Journal, 18

## All Authors and Affiliations


Daniel Huber[1,2] Ditte Slumstrup[3,4] Marc Hon[5,1] Yaguang Li[1] Victor Aguirre Børsen-Koch,[6] Timothy R. Bedding[2] Meridith Joyce[7,8] J. M. Joel Ong,[1] Aldo Serenelli,[9,10] Dennis Stello[11,2,12] Travis Berger[13] Samuel K. Grunblatt[14] Michael Greklek-McKeon[15] Teruyuki Hirano[16,17] Evan N. Kirby[18] Marc H. Pinsonneault[19] Arthur Alencastro Puls,[20] and Joel Zinn[21]

[1] *Institute for Astronomy, University of Hawai'i, 2680 Woodlawn Drive, Honolulu, HI 96822, USA*

[2] *Sydney Institute for Astronomy (SIfA), School of Physics, University of Sydney, NSW 2006, Australia*

[3] *European Southern Observatory, Alonso de Cordova 3107, Vitacura, Chile*

[4] *Instituto de Estudios Astrofísicos, Facultad de Ingeniería y Ciencias, Universidad Diego Portales, Av. Ejército Libertador 441, Santiago, Chile*

[5] *Kavli Institute for Astrophysics and Space Research, Massachusetts Institute of Technology, 77 Massachusetts Avenue, Cambridge, MA 02139, USA*

[6] *DARK, Niels Bohr Institute, University of Copenhagen, Jagtvej 128,18, 2200, Copenhagen, Denmark*

[7] *Konkoly Observatory, HUN-REN Research Centre for Astronomy and Earth Sciences, Konkoly-Thege Miklós út 15-17, H-1121, Budapest, Hungary*

[8] *CSFK, MTA Centre of Excellence, Budapest, Konkoly-Thege Miklós út 15-17, H-1121, Budapest, Hungary*

[9] *Institute of Space Sciences (ICE, CSIC), Carrer de Can Magrans S/N, Campus UAB, Cerdanyola del Valles, E-08193, Spain*

[10] *Institut d'Estudis Espacials de Catalunya (IEEC), 08860 Castelldefels (Barcelona), Spain*

[11] *School of Physics, University of New South Wales, NSW 2052, Australia*

[12] *ARC Centre of Excellence for All Sky Astrophysics in Three Dimensions (ASTRO-3D)*

[13] *Space Telescope Science Institute, 3700 San Martin Drive, Baltimore, MD 21218, USA*

[14] *William H. Miller III Department of Physics and Astronomy, Johns Hopkins University, 3400 N Charles St, Baltimore, MD 21218, USA*

[15] *Division of Geological and Planetary Sciences, California Institute of Technology, Pasadena, CA, 91125, USA*

[16] *Astrobiology Center, 2-21-1 Osawa, Mitaka, Tokyo 181-8588, Japan*

[17] *National Astronomical Observatory of Japan, 2-21-1 Osawa, Mitaka, Tokyo 181-8588, Japan*

[18] *Department of Physics and Astronomy, University of Notre Dame, 225 Nieuwland Science Hall, Notre Dame, IN 46556, USA*

[19] *Department of Astronomy, The Ohio State University, Columbus, OH 43210, USA*

[20] *Goethe University Frankfurt, Institute for Applied Physics, Max-von-Laue-Str. 12, 60438, Frankfurt am Main, Germany*

[21] *Department of Physics and Astronomy, California State University, Long Beach, Long Beach, CA 90840, USA*